Wei, G., Chen, B., Lai, D., and Chen, Q. 2020. "An improved displacement ventilation system with diffuses around columns and overhead radiant panels for a machining plant," *Atmospheric Environment*, 228:117419.

# An Improved Displacement Ventilation System with Diffuses around Columns and Overhead Radiant Panels for a Machining Plant

Guanqiong Wei[1], Bingqian Chen[1], Dayi Lai[2*] and Qingyan Chen[3]

[1]School of Environmental Science and Engineering, Tianjin University, Tianjin 300072, China
[2]Department of Architecture, Shanghai Jiao Tong University, Shanghai 200240, China
[3]School of Mechanical Engineering, Purdue University, West Lafayette, IN 47905, USA

[*]*Corresponding email: dayi_lai@sjtu.edu.cn*

**Keywords**: Indoor air quality; Thermal comfort; Experimental measurements; CFD simulation

**Abstract**

Machining plants are often highly polluted indoor environments with dense oil mist generated from metalworking fluids. Workers exposed to oil mist may suffer serious health problems. General ventilation is often used to dilute the oil mist level below the threshold of health risk. However, it is not easy to organize the flow for ventilating a large machining plant with hundreds of machines in order to effectively remove the oil mist. In order to develop an effective ventilation system, this study validated a computational fluid dynamics (CFD) program with the RNG $k$-$\varepsilon$ model at a high Grashof number by using the measured air temperature and contaminant concentration in several locations in a high-ceiling lab with heat and pollutant sources. Next, the validated CFD program was used to develop an improved displacement ventilation system in which air is supplied from the lower parts of the support columns in the plant. With thermal plumes generated by machines and workers, the system formed unidirectional airflow that carried pollutants away from the work area of the factory. The system reduced the oil-mist concentration by more than 70% compared with existing ventilation system. In addition, suspended radiant heaters are recommended for supplemental heating in winter.

## 1. Introduction

Oil mists are typical pollutants in machining factories. Metalworking fluid is used to cool and lubricate metal components during cutting, grinding and boring operations, and these processes generate oil mist through evaporation, condensation and atomization (Adler et al., 2006). Previous studies (Eisen et al., 2001; Lacasse et al., 2012; Mirer, 2010; O'Brien, 2003; Rim and Lim, 2014; Woskie et al., 1994) found that exposure to oil mist may lead to hypersensitivity pneumonias, lipoid pneumonia, lung cancer,

laryngeal cancer, asthma, bronchial hyper responsiveness, and other illnesses. To reduce the potential health risk associated with metalworking fluids, National Institute for Occupational Safety and Health (NIOSH) has limited occupational exposure to metalworking fluid aerosols to 0.5 $mg/m^3$. Moreover, cleaner indoor air can improve productivity (Fisk and Rosenfeld, 1997). However, pollutant levels in many factories have been found to exceed the above level (Zhang and Long et al., 2016; Zhang and Shao et al., 2016). Therefore, it is necessary to reduce the oil-mist concentration in machining factories.

The reduction of oil-mist concentration in a factory can be achieved by three main approaches: source elimination (Byrne and Scholta, 1993), local exhaust (Goldfield, 1985) or local purification (Mead-Hunter et al., 2014), and dilution by ventilation (Goldfield, 1985). However, source elimination may not be always possible. Local exhaust or local purification is effective only in close proximity to the machines. Furthermore, local exhaust is difficult in a non-enclosure or conventional milling machinery environment (Chia et al., 2019). Therefore, diluting the oil-mist concentration by ventilation is the most widely used approach in industrial settings. Two types of ventilation systems (Cao et al., 2014) are commonly employed: mixing ventilation and displacement ventilation. A mixing ventilation system (Boyle, 1899) is used to mix air as thoroughly as possible in order to create uniform air temperature and pollutant concentration distributions. Because a machining plant often has a very wide span and very high ceiling, mixing ventilation in this setting uses jets with very high supply air velocity. Unfortunately, a well-mixed state is hard to achieve. Displacement ventilation supplies cool air at floor level and extracts air at ceiling level, creating a unidirectional upward airflow due to thermal buoyancy from heat sources (Yuan et al., 1999). As a result, there are air temperature and contaminant stratifications (Li et al., 1992).

Previous studies found that displacement ventilation was appropriate for large spaces such as factories. Breum and Skotte (1992) compared the temperature distribution between mixing and displacement ventilation in a factory and found that displacement ventilation would form temperature stratification. Moon et al. (2005) compared displacement ventilation with mixing ventilation in a factory and found that displacement ventilation can remove pollutants more effectively than mixing ventilation, especially for small particle sizes (Chakroun et al., 2019). Wang and Huang et al. (2012) studied displacement ventilation in a fume factory with high-power heat sources. They found that upward thermal plumes can

remove particles very effectively. In previous studies, traditional displacement ventilation diffusers were usually installed on perimeter walls. In practical application, air discharged through these diffusers may not have reached the core spaces in a factory, which could have 100 m span (Zhang and Long et al., 2016). Lau and Chen (2007) used an underfloor air distribution system to remove gaseous pollutants in a small workshop. The system was effective in removing pollutants. However, the floor of a large machining factory can be dirty, and it must be able to support the heavy weight of moving vehicles. An underfloor air distribution system may not be practical. Therefore, this paper reported our effort in developing an improved displacement system for a factory that can deliver air anywhere in the factory where ventilation is needed.

## 2. Object description

This study took an actual machining factory as the research object. To solve the oil mist pollution mentioned above, this study improved displacement ventilation system with diffusers installed around the lower parts of the support columns in a large machining plant. Infrared radiant heaters were installed to supply heat. The existing ventilation system and the proposed ventilation system in the machining factory would be modeled as followed.

The machining plant with high oil-mist pollutant levels was chosen for the study, in which car components were manufactured. As shown in Figure 1, the machining plant was 206 m long, 90 m wide, and 8 m high. The plant contained many production lines, each composed of two rows of equipment with a narrow aisle of about 1.5 m. Most of the equipment was about 2.5 m high and semi-automatic in operation, but workers needed to be in the aisles when the equipment was operational. The equipment emitted much fewer oil mist when the machine lids were closed than when the lids were open. The oil mist pollution in the machining plant was high. Figure 1(b) shows the existing ventilation system of the machining plant. The circulation system took in the contaminated air at mid-height, filtered it, and returned the clean air downward into the plant. Large amounts of outdoor air infiltrated into the factory around the doors and windows. The exhaust fans on the ceiling also extracted contaminated air. But with the existing ventilation system, the pollution of oil mist was still seriously.

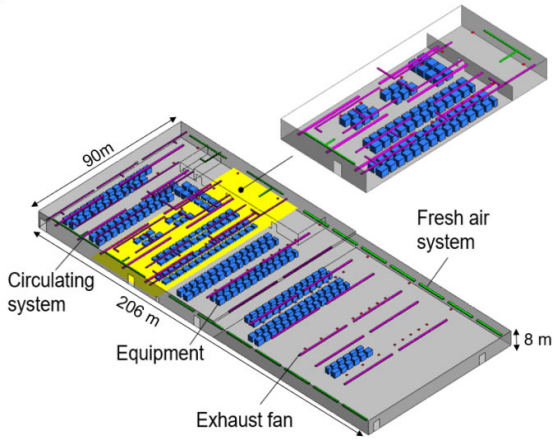


*(a)*

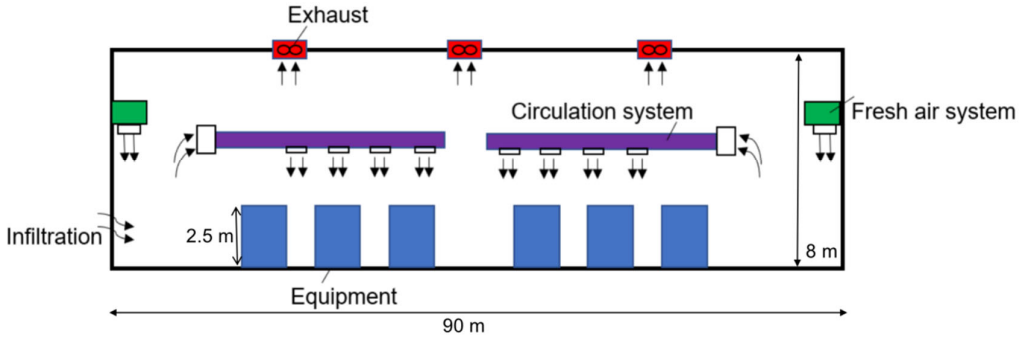


*(b)*

*Figure 1. (a) Sketch of the machining plant with existing ventilation system and (b) the details of the existing ventilation system (Please note the dimension was not scaled so it was illustrative).*

Figure 2 illustrates the proposed ventilation system for the machining plant. Different from traditional displacement ventilation system, the orientation of diffusers was all around. The diffusers installed around the lower parts of the support columns in a large machining plant. The columns were originally designed to support the roof and were uniformly distributed throughout the plant. This improved ventilation system can thus deliver cool, clean air to all the spaces within the plant. The negative buoyancy from the cool air causes the clean air to remain at floor level. Thermal plumes from the heat sources in the plant, such as machines, can carry the pollutants generated in the occupied zone to the upper region of the plant. The polluted air in the upper region is then exhausted to the outdoor environment through the ventilation outlet as Figure 2(b) showed. Since a displacement ventilation system always provides cool air to a space, winter heating requires an additional system. Our system uses

overhead infrared radiant heaters, which can be installed in work spaces that require heating.

The improved ventilation system did not use the circulation system, and the supply airflow rate was the same as the exhaust rate in the original system. Table 1 provides the air supply information, and Table 2 the surface temperature and oil-mist source information for the plant. Unlike the existing system, which supplied warm air in winter, the improved system supplied cool air in winter but used local infrared heaters to provide thermal comfort to the workers. All other thermal and fluid boundary conditions remained the same between the two systems, as shown in Tables 1 and 2.

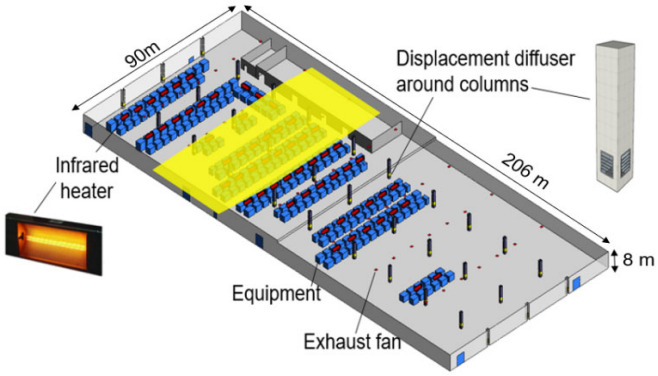


*(a)*

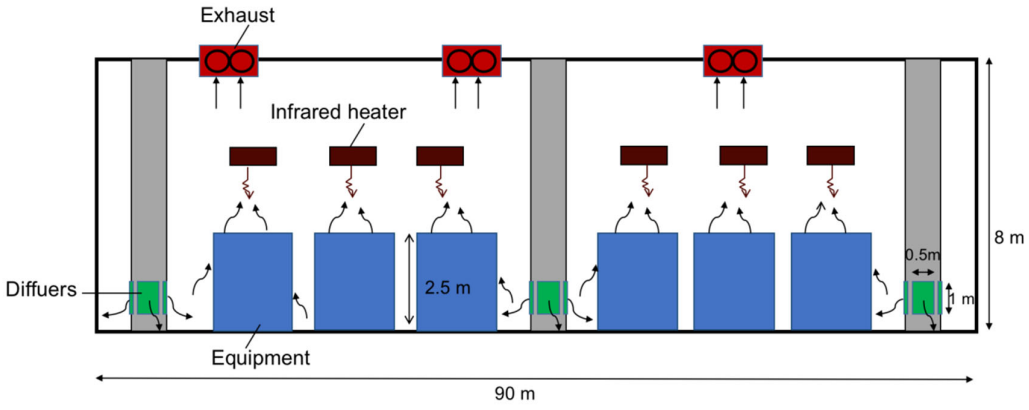


*(b)*

*Figure 2. (a) Sketch of the machining plant with the improved ventilation system and infrared heaters and (b) the details of the improved ventilation system.*

Table 1. *Air supply parameters of existing and improved ventilation systems.*

| | | Existing ventilation | Improved ventilation |
|---|---|---|---|
| Supply air volume ($m^3/s$) | | 253 | 253 |
| Supply temperature (°C) | Winter | 32 | 18 |
| | Summer | 22 | 22 |

Table 2. *Surface temperatures in the plant and particle source information.*

| | | Winter | Summer |
|---|---|---|---|
| Surface temperature (°C) | Wall | 20 | 33 |
| | Equipment | 21 | 35 |
| | Floor | 19 | 33 |
| | Roof | 21 | 39 |
| Oil-mist source | Oil mists (particles) generated by each piece of equipment (kg/s) | $2.8\times10^{-7}$ | |
| | Oil mist density ($kg/m^3$) | 800 | |

The highlighted zone in Figures 1(a) and 2(a) was used for modeling and comparing the two systems because the highlighted zone was the most heavily polluted area. Gambit (2005) was used to generate the unstructured tetrahedral cells for both cases. Meshes were finer near the supply, outlet and walls with a minimum size of 0.1 m and the growth rate no more than 1.1. A total of 2.9 million cells was used for the space with the existing ventilation system and 2 million for that with the improved ventilation system. The grid dependence for each case was checked by doubling the number of cells, until no more than 20% of difference in velocity was achieved between former and later simulations.

## 3. Method

To evaluate the proposed ventilation system, this study compared the distributions of air velocity, air temperature and oil-mist concentration with those created by existing ventilation system and the proposed ventilation system by numerical simulation. An experiment was also conducted in a high-ceiling lab to validate the numerical method.

### 3.1 CFD modeling

#### *3.1.1 Model for fluid phase*

To evaluate the improved displacement ventilation system, we studied its effect on oil-mist dilution and temperature distributions in machining plants. Two methods are typically used to evaluate a ventilation system: experimental measurements and computer simulations. It is very challenging to conduct experimental measurements in an actual factory with sufficient spatial resolution. A reduced-scale model using water is an alternative(Lin and Lin, 2014; Lin and Wu, 2017), but it would be hard to achieve similarity when inertial and buoyancy forces are comparable. Computer simulations, such as the computational fluid dynamics (CFD) technique, can provide valuable information, and a variety of cases can be easily simulated (Wang and Zhai, 2016). Hence, this investigation used the CFD technique (Nielsen, 1974) to evaluate the performance of the proposed displacement ventilation system.

Generally, CFD predicts turbulent flows by three methods: direct numerical simulation (DNS), large eddy simulation (LES), and Reynolds-averaged Navier-Stokes (RANS) equation simulation with turbulence models. Zhai et al. (2007) has shown that DNS and LES are accurate and can provide very valuable information about flow. However, DNS and LES would require a high-capacity computer and long computing time if they were used to simulate a large factory. Meanwhile, RANS models calculate Reynolds-averaged variables of flow and model turbulent flow to reduce computing time. Zhang et al. (2007) have shown that for indoor airflow simulation, some RANS models, such as the renormalization group (RNG) $k$-$\varepsilon$ model (Choudhury, 1973; Wang and Chen, 2009; Yakhot and Orszag, 1986), perform with reasonable accuracy, computational cost and robustness. Hence, the RNG $k$-$\varepsilon$ model in the commercial CFD software ANSYS Fluent (ANSYS, 2017) was selected for our study.

The numerical simulations used the SIMPLE algorithm (Patankar, 2018) to solve the discretized governing equations. Second-order upwind schemes were used for all the variables except the pressure, for which a staggered PRESTO! scheme was employed. A simulation was considered to be converged when the net mass and energy balances were less 1‰ of the sum of the absolute normalized residuals for all the cells in the flow domain.

Although numerous researchers (Chen, 1995; Zhang et al., 2007) have recommended the RNG $k$-$\varepsilon$ model as having good overall performance among the available RANS models for indoor environments, the model uses many assumptions in order to solve turbulent flow. The results obtained by CFD simulations with the model may not be correct, and they must be validated by corresponding experimental data.

*3.1.2 Eulerian and Lagrangian models for oil mist dispersion*

For oil-mist transport in a machining plant, the oil volume is usually a very small fraction of the total air volume. Thus, the influence of the oil mist on turbulent flow is negligible; one usually studies the impact of airflow on oil-mist distribution, and not the other way around (Holmberg and Li, 1998). To study the one-way impact of airflow on oil mist, this investigation used both the Eulerian and Lagrangian methods. The Eulerian method treats oil-mist flow as a continuum and calculates the oil-mist concentration in the space. The Lagrangian method considers oil mist as discrete particles and tracks the pathways of individual particles.

The concentration equation calculated within the Eulerian method can be written as:

$$\partial C_p / \partial t + \nabla(C_p \vec{u}_m) = -\nabla(C_p \vec{v}_{dr,p}) \tag{1}$$

where $C_p$ is particle concentration, $\vec{u}_m$ is the mass-averaged velocity, and $\vec{v}_{dr,p}$ is the drift velocity for the particle phase. Here $\vec{u}_m$ is in the following form:

$$\vec{u}_m = \left(\alpha_p \rho_p \vec{u}_p + \alpha_a \rho_a \vec{u}_a\right) / \rho_m \tag{2}$$

where $\alpha_p$ is the volume fraction of particles, $\alpha_a$ the volume fraction of air, $\rho_p$ particle density, $\rho_a$ air density, $\rho_m$ mixture density, $\vec{u}_p$ particle velocity, $\vec{u}_a$ air velocity, and $\vec{v}_{dr,p}$ takes the following form:

$$\vec{v}_{dr,p} = \vec{u}_p - \vec{u}_m \tag{3}$$

The Lagrangian method calculates the trajectory of a discrete phase particle by using Newton's law:

$$d\vec{u}_p / dt = F_D \left(\vec{u}_a - \vec{u}_p\right) + \vec{g}(\rho_p - \rho_a) / \rho_p + \vec{F}_a \tag{4}$$

where $F_D$ is the inverse of relaxation time, $\vec{g}$ gravity acceleration, and $\vec{F}_a$ additional force. The first term on the right-hand side is the drag term, the second term represents the gravity and the buoyancy,

and the third term stands for other forces on the particles. The drag force is the most significant and follows Stokes' drag law:

$$\vec{F}_{drag} = F_D(\vec{u}_a - \vec{u}_p) = {}^{18\mu}\!/_{\rho_p d_p^2 C_c}(\vec{u}_a - \vec{u}_p) \quad (5)$$

where $\mu$ is air viscosity, $d_p$ particle diameter and $C_c$ the Cunningham correction factor. A comparison of orders of magnitude indicates that other forces such as the Basset history, the pressure gradient, the virtual mass, Brownian, thermophoretic and Saffman's lift forces are infinitesimal and negligible in relation to the drag force (Li and Ahmadi, 1992).

The $\vec{u}_a$ includes two components, average velocity and instantaneous velocity. The former is obtained by solving the RANS equations, and the latter needs to be modeled by the discrete random walk (DRW) model. In the DRW model, the instantaneous velocities follow the Gaussian distribution, and they are correlated with the flow turbulent kinetic energy:

$$u'_i = \xi_i\sqrt{2k/3} \quad (6)$$

where $u_i'$ is instantaneous velocity, $k$ is the turbulent kinetic energy, and $\xi_i$ is a normally distributed random number.

The Lagrangian method calculates the particle trajectories instead of particle concentration. Therefore, this study employed user-defined functions to calculate concentration distribution from the trajectories (Zhang and Chen, 2006).

Besides the comparison of raw data of temperature and contaminant concentration distribution, the paper also compared the ventilation effectiveness of both systems through the contaminant removal effectiveness. The study used the contaminant removal effectiveness $\eta$, which defined as Equation (7) (Nielsen et al., 2004), to evaluate the system.

$$\eta = \frac{c_e - c_s}{c - c_s} \quad (7)$$

where $c_e$ is the contaminant concentration in the exhaust, $c$ is the mean contaminant concentration at 1.5 m above the floor, $c_s$ is the contaminant concentration in the supply air.

**3.2 Experimental methodology**

As discussed above, the CFD simulation used approximations, and thus there may be some uncertainty in the results. Hence, it was necessary to validate the CFD model before it could be used to study the ventilation system (Chen and Srebric, 2002). This validation required experimental data on airflow with similar flow features. Ideally, we would have used experimental data from a machining plant. However, in our literature search, we did not find any such data. The experimental data on displacement ventilation was always obtained in indoor spaces with a low ceiling height of about 3 m. The corresponding Grashof numbers in these indoor spaces were lower than those in machining plants, which usually have high ceilings. Therefore, this study used a room with a high ceiling, as shown in Figure 3, to obtain experimental data. This room had a comparable Grashof number ($10^{11}$ magnitude) to that in an actual machining plant, and thus the flow would also be similar.

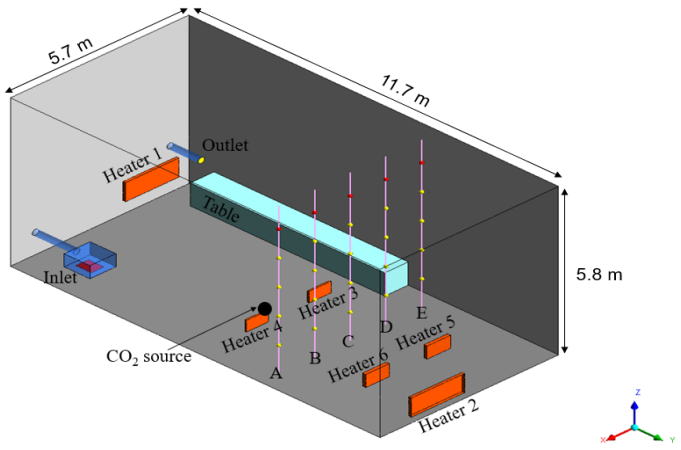


*Figure 3. Room sketch and measuring positions.*

The room used for the tests was 11.7 m long, 5.7 m wide and 5.8 m high. Table 3 lists the surface temperatures of the room. To mimic winter heating conditions, this investigation placed six heaters in different parts of the room as shown in Table 4. The table also provides the surface temperatures of the heaters. Both the air supply inlet and exhaust outlet were in the lower part of the room. As the inlet duct was small, the air velocity in the duct was high up to 7.5 m/s. If the air was supplied directly to the room, the inlet jet would be very strong and would reach the other end of the room at high speed. In that case, the flow features in the room would not be those of displacement ventilation. Therefore, this investigation connected a pressure box to the air supply inlet. The air was supplied downward through the bottom

opening of the box, as indicated by the red area on the inlet in Figure 3. As a result, the airflow features in the room were similar to those of displacement ventilation. The air was supplied at a temperature of 10.9°C and 1.35 m/s for a rate of 850 $m^3$/h or 2.2 ACH (air change rate per hour). $CO_2$ was used as a tracer gas; it was released at a rate of 20 L/min and at a height 0.55 m above the floor. Air temperature was measured in five positions (poles A through E) at heights of 1, 2, 3, 4, and 5 m above the floor, and $CO_2$ concentration was measured in these five positions at heights of 1, 2, 3, and 4 m above the floor.

Table 3. Surface temperatures in the room.

| Boundary | Temperature (°C) |
|---|---|
| North wall (+y) | 19 |
| South wall (-y) | 19 |
| East wall (+x) | 17.7 |
| West wall (-x) | 19 |
| Floor (-z) | 15.5 |
| Ceiling (+z) | 18 |

Table 4. Heaters used in the room.

| Heat | Position | | | Size | | | Surface temperature |
|---|---|---|---|---|---|---|---|
| source | x (m) | y(m) | z (m) | Δx (m) | Δy (m) | Δz (m) | °C |
| Heater 1 | 0.4 | 0 | 0.46 | 1.7 | 0.08 | 0.66 | 32 |
| Heater 2 | 3 | 11.72 | 0.2 | 1.7 | 0.08 | 0.66 | 34 |
| Heater 3 | 1.5 | 5.985 | 0 | 0.7 | 0.05 | 0.4 | 210 |
| Heater 4 | 3.5 | 5.985 | 0 | 0.7 | 0.05 | 0.4 | 220 |
| Heater 5 | 1.5 | 9.75 | 0 | 0.75 | 0.1 | 0.45 | 100 |
| Heater 6 | 3.45 | 9.75 | 0 | 0.75 | 0.1 | 0.45 | 100 |

Before the start of each measurement, the room was ventilated for 4 h to reach a thermally steady-state condition. Next, $CO_2$ was released for 1.5 h to ensure a species transport steady-state condition. The air temperature was then measured by a K-style thermocouple with an accuracy of ±1.5 K, and $CO_2$ concentration by an infrared carbon dioxide sensor Telaire-7001 with an accuracy of ±5% ppm. The

surface temperature was measured by an infrared camera with an accuracy of ±1K.

## 4. Results

### 4.1 CFD model validation

This investigation used the CFD model mentioned above to simulate the air distribution in the room. Gambit (2005) was used to generate unstructured tetrahedral gird. The minimum size was 0.03 m, the maximum size 0.18 m and the growth rate was no more than 1.15 with a total of 1.3 million cells. Figure 4 compares the simulated air temperature and $CO_2$ concentration profiles along the five poles with the corresponding experimental data. The temperature and $CO_2$ profiles were typical for displacement ventilation. Thus, the airflow features in the room were indeed close to those of displacement ventilation. The results demonstrate that the model can predict the air temperature with high accuracy. For $CO_2$ concentration, the simulated results agree in general with the experimental data, but with a maximum difference of 12%. The large error observed at 1 m above the floor along pole A may have been caused by the strong turbulence there. The average error of $CO_2$ concentration was 6.3%. Overall, the comparison indicates that the RNG *k-ε* model can predict air distribution in a high-ceiling room with displacement ventilation.

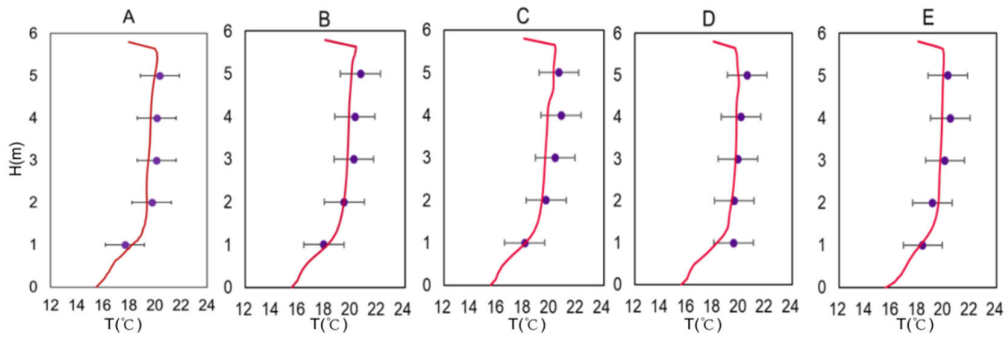


*(a) air temperature*

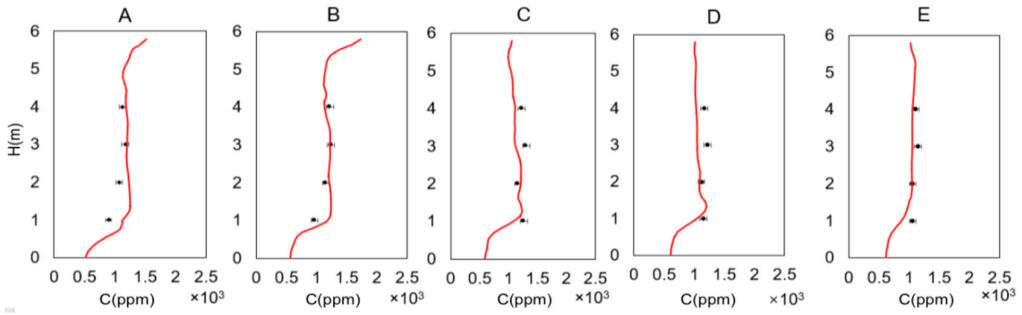


*(b) $CO_2$*

*Figure 4. Comparison of computed air temperature and $CO_2$ profiles along poles A through E with the corresponding experimental data. Symbols – data; lines – computed results.*

## 4.2 Evaluation of the improved ventilation system

### *4.2.1 Comparison of the existing and improved ventilation systems in summer*

Figure 5 depicts the airflow distribution in a vertical section through the air recirculation system of the existing ventilation system in summer. The existing system created many large vortexes between the machines and the jets of the recirculation system because of the opposing airflow directions. The recirculation system blew air downward, while the thermal plumes from the machines traveled upward. The airflow in the plant was poorly organized, and the oil mist was trapped in the vortexes. In addition, airflow above the recirculation system was of very low velocity because the exhaust fans did not significantly affect the airflow in this region.

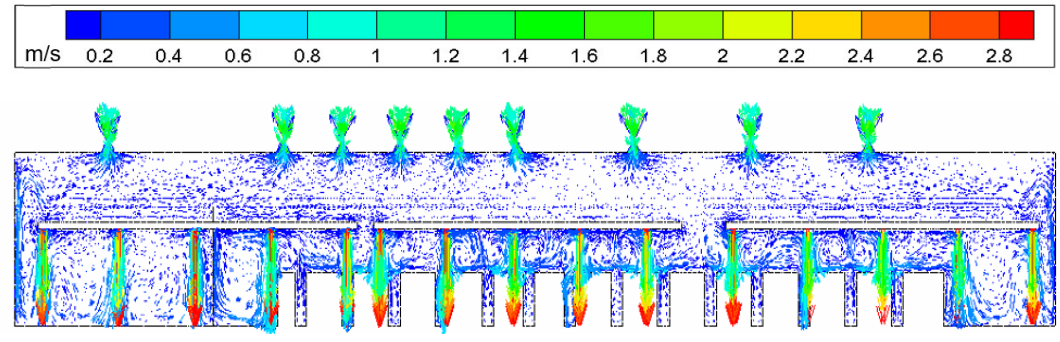


*(a) Existing system*

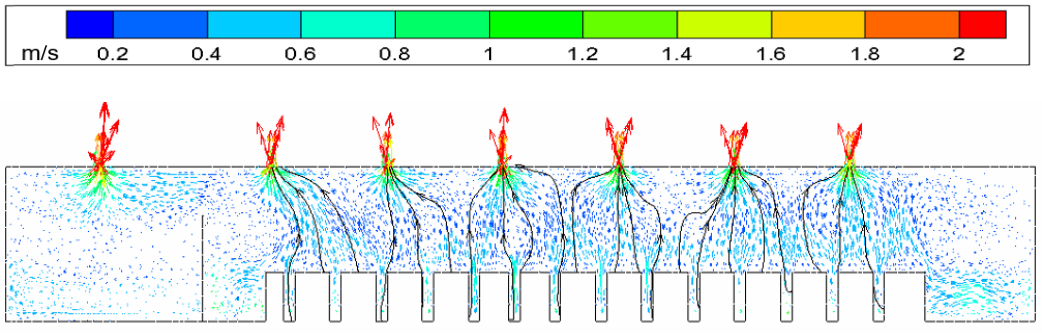


*(b) Improved system*

*Figure 5. Comparison of the air distribution in vertical section for two ventilation systems in summer.*

The improved system supplied cool air through the column diffusers to the lower part of the plant. Since the supply air was cooler than the air in the plant, negative buoyancy would keep the supply air in the lower part of the plant. The air would then be gradually heated by the machines, and the oil mist would be transported to the upper part of the plant by the thermal plumes formed by the machines, as shown in Figure 5(b). Finally, the oil-mist-contaminated air would be exhausted to the outside environment by the fans on the roof.

Figure 6 illustrates the temperature distributions in the vertical section for the two ventilation systems. The existing system created a fairly uniform air temperature distribution in the lower part of the room. This occurred because the supply air from the recirculation system and thermal plumes from the machines interacted to form a mixed condition. In the upper part of the plant, the air was stratified because of the low air velocity there. In contrast, the improved system formed a stratified air temperature distribution from the floor to the ceiling, which is typical for displacement ventilation. The temperature difference between head and foot level was about 1.9 K. At the same supply air temperature, the air temperature in the plant near the floor was lower than that with the existing system. This finding indicates that the air temperature in the occupied zone with the improved system was cooler than that with the existing system, which could provide additional comfort to the workers in summer.

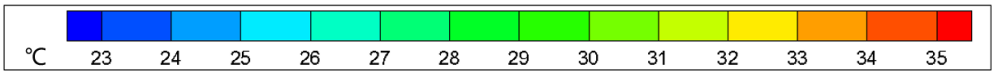

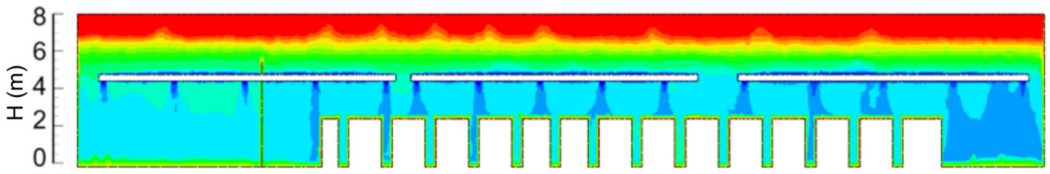


*(a) Existing system*

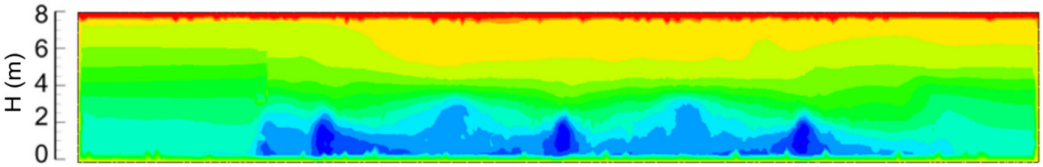


*(b) Improved system*

*Figure 6. Comparison of the air temperature in vertical section for the two ventilation systems in summer.*

This investigation used both the Eulerian and Lagrangian methods to simulate the oil-mist concentration distribution in the plant. Since the oil-mist concentration in the breathing zone was more concerned, so we firstly compared the horizontal plane at a height of 1.5 m above the floor. As shown in Figure 7, the two methods predicted similar oil-mist concentration distributions in the breathing zone horizontally. The average facet error between these two methods was 9.9%. The distribution by the Lagrangian method was more scattered because a limited number of particles were released in the simulation. We also measured the oil-mist concentration in five locations at 1.5 m above the floor, as illustrated in Figure 7(a). The oil-mist concentration was measured by TSI 8530 with an accuracy of ± 0.1%. Comparison with the experimental data in Figure 7(c) again confirms that the two methods can predict the oil-mist concentrations with reasonable accuracy.

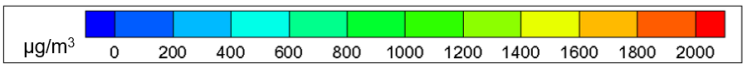

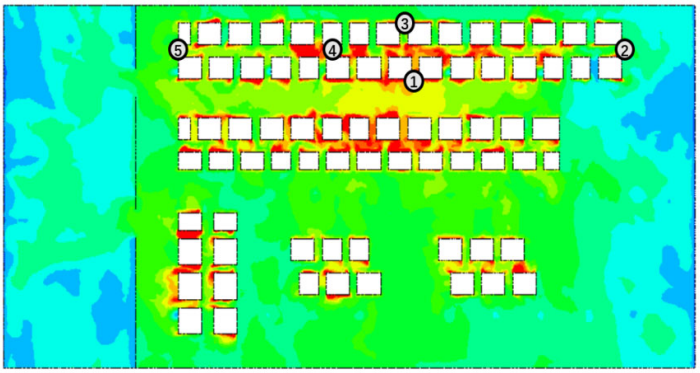


*(a) Eulerian method for the existing system*

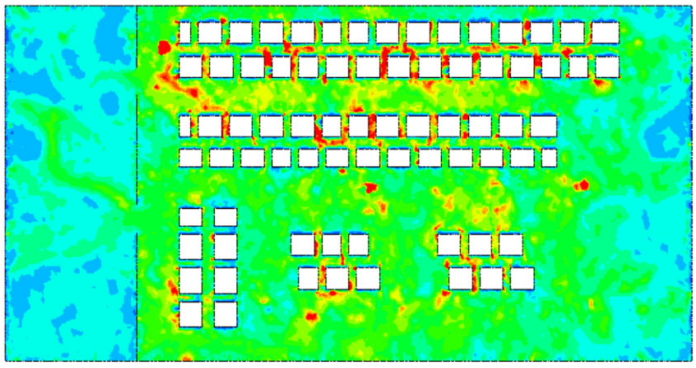

*(b) Lagrangian method for the existing system*

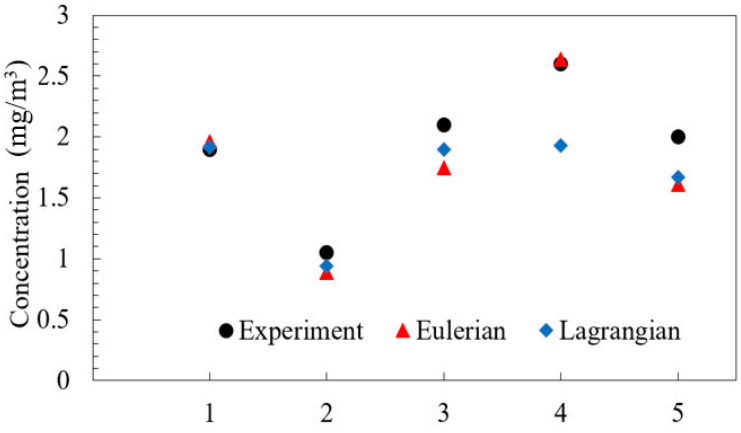


*(c) Comparison with experimental data on oil-mist concentration in five locations for the existing system.*

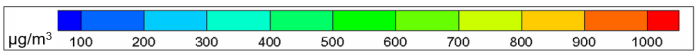

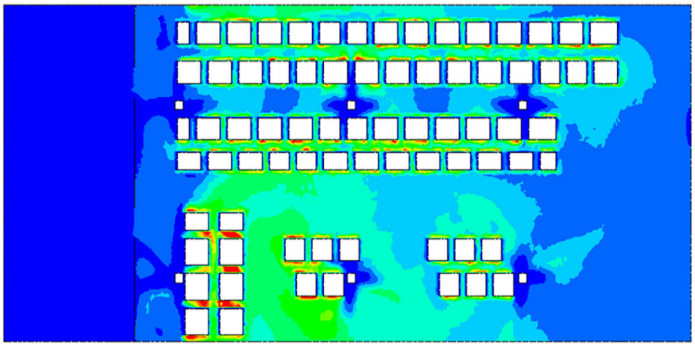

*(d) Eulerian method for the improved system*

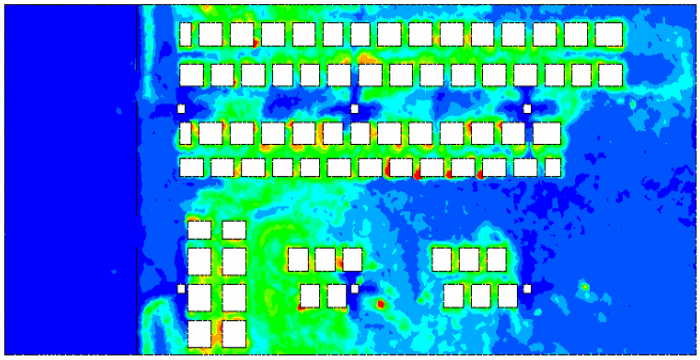

*(e) Lagrangian method for the improved system*

*Figure7. Comparison of oil-mist concentration distribution at 1.5 m above the floor for two ventilation systems in summer.*

Figure 7(d) and (e) depict the oil-mist concentration distributions with the improved ventilation system calculated by the Eulerian and Lagrangian methods, respectively. The average facet error between these two methods was 2.4%. The oil-mist concentration was much lower than that with the existing system. In this figure, the concentration is represented by a color scale, as shown in the legends. The average concentration along this plane was reduced from 1,062 $\mu g/m^3$ with the existing system to 248 $\mu g/m^3$ with the improved system. This 76% reduction is remarkable. The extremely low ventilation effectiveness as 0.11 with the existing system because of the poor organization of airflow. And the ventilation effectiveness of the improved system was 2.8 as displacement ventilation system was always above 1. Since the two methods yielded similar results for the improved system, the Eulerian method has been used to calculate the results in the remainder of the paper.

Next, Figure 8 compares the oil-mist concentration with the two systems in the vertical-cross section

through the air recirculation system. As demonstrated in the previous paragraph, the improved ventilation system dramatically reduced the oil-mist concentration. Again, one should note the color scale in the legend. When the oil-mist concentration in Figure 8(a) is compared with the airflow in Figure 5(a), it can be seen that the vortexes trapped considerable amounts of oil mist in the middle of the plant. The existing system created a suspended oil-mist zone that was not observed with the improved system. This suspended zone was located at breathing level.

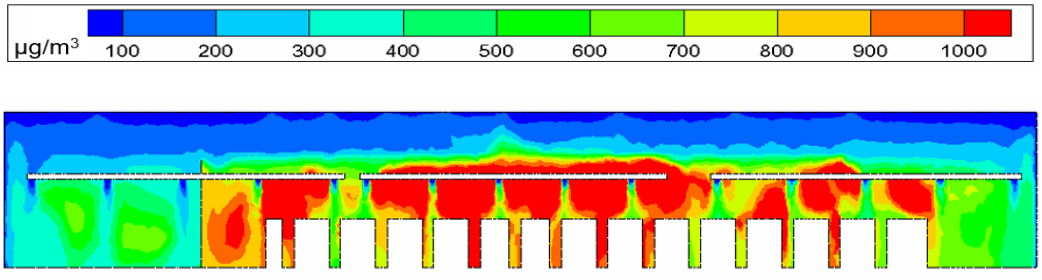


*(a) In the section through the air-recirculation system for the existing system*

*(b) In the same section for the improved system*

*Figure 8. Comparison of oil-mist concentration distribution in vertical section for two ventilation systems in summer.*

*4.2.2 Comparison of the existing and improved ventilation systems in winter*

Figure 9(a) illustrates the airflow distribution in a vertical section through the air recirculation system of the existing ventilation system in winter. The air jets in the existing system did not extend as far in winter as in summer, because of buoyancy. The vortexes in winter were smaller than in summer because of weaker interaction. The warm air tended to move upward, as did the thermal plumes from the heated equipment. Because of this upward airflow, the velocity in the upper part of the factory in winter was higher than that in summer. As shown in Figure 9(b), the airflow distribution with the improved system in winter was similar to that in summer. This occurred because the column diffusers still supplied cool

air in winter in order to produce displacement ventilation. The airflow distribution with the improved system was much better organized than with the existing system.

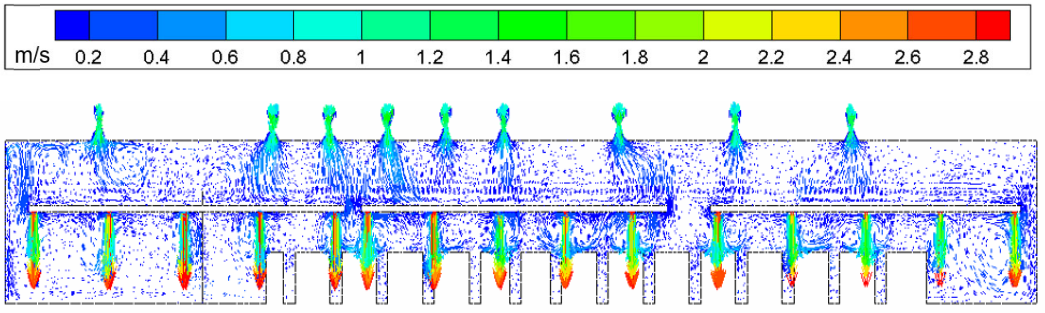


(a) *Existing system*

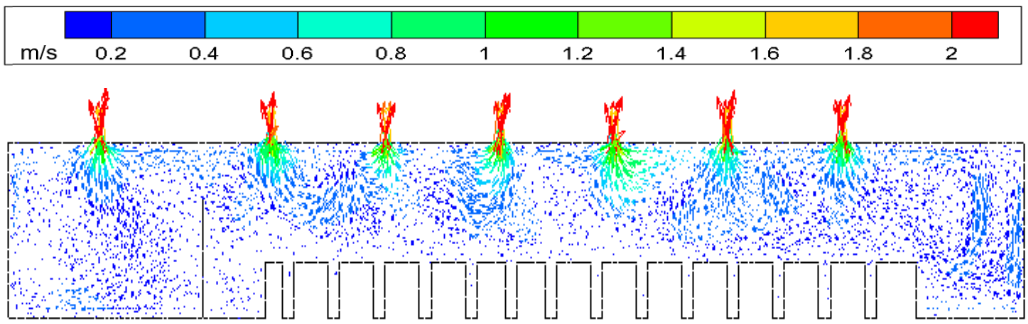


*(b) Improved system*

*Figure 9. Comparison of the air distribution in vertical section for two ventilation systems in winter.*

Figure 10(a) depicts the temperature distribution in the vertical section through the air recirculation system of the existing ventilation system in winter. In contrast with the situation in summer, the air temperature distribution was uniform in both the lower and upper parts of the plant because the upward-flowing warm supply air facilitated mixing in the upper part. Meanwhile, the improved ventilation system still maintained displacement ventilation, and thus temperature distribution was stratified. However, the supply air temperature needed to be lower than the room air temperature. The mean air temperature in the occupied zone was only 18°C. The temperature difference between head and foot level was about 0.8 K. To improve thermal comfort in winter, overhead infra-red heat panels should be installed at a height of 5 m above the flow. The panels would provide heat to the workers mainly by radiation. Although the air in the work area would be heated only slightly by the panels, this would be sufficient to maintain the

same operating temperature as that provided by the existing ventilation system in winter.

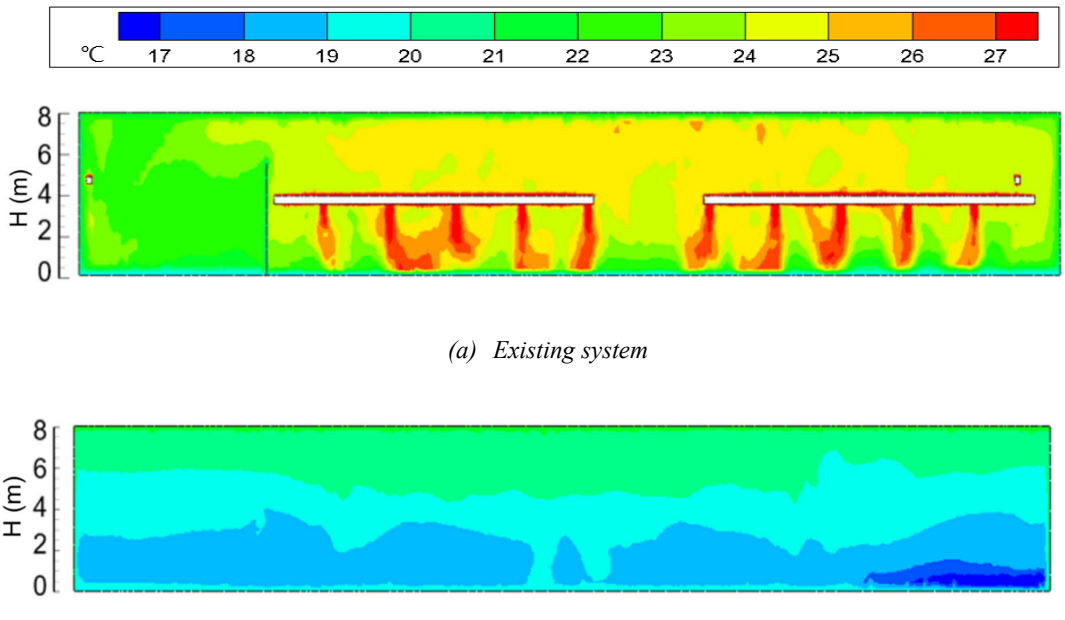


*(a) Existing system*

*(b) Improved system*

*Figure 10. Comparison of the air temperature in vertical section for the two ventilation systems in winter.*

Figure 11 compares the oil-mist concentration in the breathing zone for the two systems in winter. The average concentration along this plane was 904 μg/m$^3$ for the existing system, which was similar to that in summer. However, the oil-mist distribution was quite different. In winter, when the air was not as well mixed, the oil mist was more likely to collect in the work area than disperse throughout the factory. Unlike the conflicting airflow pattern for summer situation, the ventilation effectiveness in the winter was higher than that in summer at 0.65. Meanwhile, the oil-mist concentration with the improved system was 280 μg/m$^3$ and the ventilation effectiveness of the improved system was 2.6, which was almost the same as that in summer. A comparison of the two systems in winter indicates a 70% reduction in oil-mist concentration with the improved system.

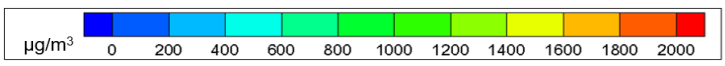

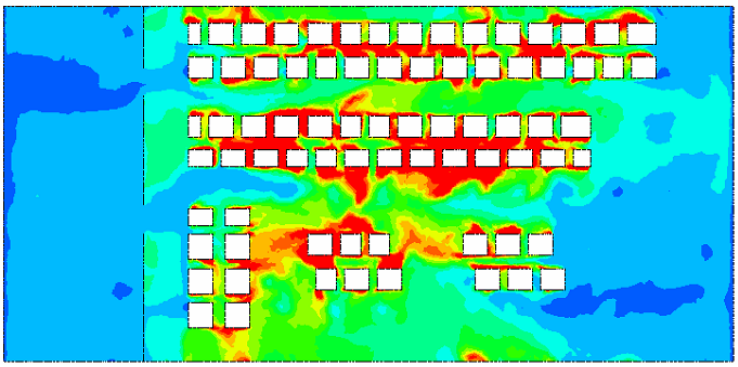

*(a) Existing system*

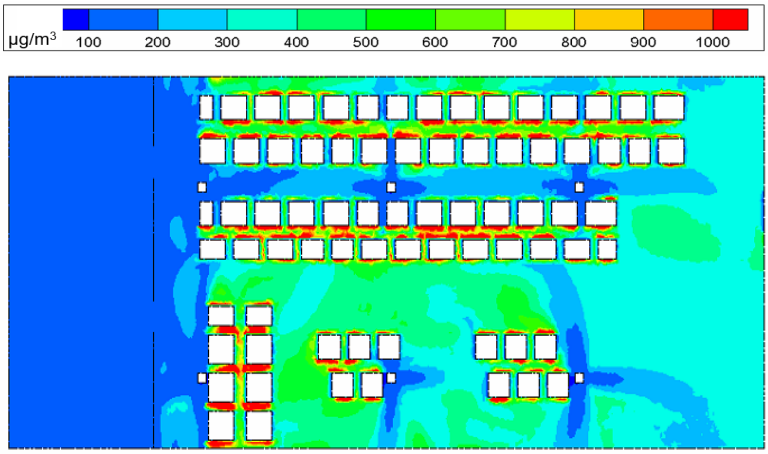


*(b) Improved system*

*Figure 11. Comparison of oil-mist concentration distribution at 1.5 m above the floor for two ventilation systems in winter.*

## 5. Discussion

The simulation involved limitations in two areas: flow fields and particle distributions.

In regard to flow fields, our on-site investigation found air flow rates of $1.185\times10^6$ $m^3/h$ from the recirculation ventilation system and $0.714\times10^6$ $m^3/h$ from infiltration. The infiltration rate was fairly significant. A portion of the infiltration ($0.247\times10^6$ $m^3/h$) occurred through visible cracks around doors and windows, and the remainder through invisible cracks in the walls and roof. CFD simulation can simulate the visible part of infiltration reasonably well, but not the invisible part because of the unknown locations and sizes of cracks. This investigation assumed that the visible air infiltration was distributed

evenly across the walls and roof. According to the ASHRAE fundamentals handbook (2013), the infiltration volume ratio of roof to walls is 2. The actual error associated with the simulation of infiltration is unclear.

In regard to particle distribution, although the Eulerian and Lagrangian methods led to similar particle distributions, there was still a difference. The average facet error between the two methods was 9.9% for the existing system and 2.4% for the improved system. Other researchers (Chen et al., 2015a; Wang and Lin et al., 2012; Zhang and Chen, 2007) have obtained similar results. The cause of the difference requires further study. In addition, although the Eulerian and Lagrangian methods led to similar results, the latter method usually requires more computing time (Zhang and Chen, 2007). In the present study, the computing time depended on the number of particles released during the simulation. For example, when $25\times10^3$ particles were released per time step, it took 42 minutes for our computer to calculate 100 steps. When $38\times10^3$ particles were released per step, the corresponding computing time increased to 95 minutes. If too few particles were released, the particle concentration would appear quite random and scattered. In this case, the results might not represent an average but rather a particular scenario. If too many particles were used, the computing time would be excessive. Therefore, reducing the released particles to a reasonable number was desirable. Chen et al. (2015b) proposed Equation (8) to estimate the necessary particle number and target volume. However, the method applied only to a well-mixed room. It tended to underestimate the particle number if there was obvious concentration stratification, as with our improved system of displacement ventilation. Moreover, the existing ventilation system in the present study created a suspended zone that was not well mixed. The estimation of particle number is therefore difficult. Balancing accuracy and simulation time, we injected a total of $64\times10^6$ particles in accordance with Equation (8) and the actual airflow pattern:

$$N \geq \frac{t_s}{\tau} V_{room} \Big/ \alpha\left(1 - exp\left(-\frac{t_s}{\tau}\right)\right) V_{target} \, N_{target}^{*} \tag{8}$$

The calculation ignored particle deposition, suspension and evaporation because the oil-mist diameter was small (0.7 μm). Previous studies (Boor et al., 2015; Chen and Zhao, 2010; Kukkonen et al., 1989; Li and Ahmadi, 1992; Zhao et al., 2009; Zhu et al., 2012) showed that when particle diameter was smaller than 1 μm, this negligence was acceptable.

## 6. Conclusions

This investigation proposed an improved ventilation system that created a clean breathing zone in an industrial space with a large amount of oil-mist pollution for an industrial plant with a wide space span. The study led to the following conclusions:

(1) The improved displacement ventilation system supplies air from the lower part of the support columns in a machining plant and extracts polluted air at ceiling level. The improved system can create a much cleaner occupied zone than the mixing ventilation method under both summer and winter conditions by reducing the oil-mist concentration by 76% and 70%, respectively.

(2) The improved system created a stratified flow, but the temperature difference between head and foot level was less than 1.9 K. The air temperature in the plant in winter was lower than that in summer because the system still supplied cool air. Overhead radiant panels were used to improve thermal comfort by raising the operative temperature to the same level as with the mixing system. Therefore, the improved system can provide thermally comfortable conditions in both summer and winter.

(3) Both the Eulerian and Lagrangian methods predicted the oil-mist concentration with reasonable accuracy. The results of the two methods were very similar and were comparable to data measured in several locations in the plant. Since the computing cost for the Eulerian was much lower than that for the Lagrangian method, the Eulerian method was recommended for similar applications in the future.

## ACKNOWLEDGEMENT

This study was supported by the National Key R&D Program of the Ministry of Science and Technology, China, on “Green Buildings and Building Industrialization” through Grant 2018YFC0705300.

## REFERENCES

Adler, D. P., Hii, W. W. S., Michalek, D. J., Sutherland, J. W., 2006. Examining the role of cutting fluids

in machining and efforts to address associated environment/health concerns. Mach. Sci. Technol. 10(1), 23-58.
ASHRAE Handbook: Fundamentals, 2013. American Society of Heating, Refrigerating and Air-Conditioning Engineers. Atlanta.
ANSYS Fluent, 2017. ANSYS Fluent Theory Guide. ANSYS Inc., Pennsylvania.
Boor, B. E., Spilak, M. P., Corsi, R. L., Novoselac, A., 2015. Characterizing particle resuspension from mattresses: chamber study. Indoor Air 25(4), 441-456.
Boyle, R., 1899. Natural and artificial methods of ventilation: Robert Boyle & Son, London.
Breum, N. O., Skotte, J., 1992. Displacement ventilation in industry—a design principle for improved air quality. Build. Environ. 27(4), 447-453.
Byrne, G., Scholta, E., 1993. Environmentally clean machining processes — A strategic approach. CIRP Annals 42(1), 471-474.
Cao, G., Awbi, H., Yao, R., Fan, Y., Sirén, K., Kosonen, R., Zhang, J. J., 2014. A review of the performance of different ventilation and airflow distribution systems in buildings. Build. Environ. 73, 171-186.
Chakroun, W., Alotaibi, S., Habchi, C., Ghali, K., Ghaddar, N., 2019. Comparison of removal effectiveness of mixed versus displacement ventilation during vacuuming session. Build. Environ. 155, 118-126.
Chen, C., Liu, W., Lin, C., Chen, Q., 2015a. Comparing the Markov chain model with the Eulerian and Lagrangian models for indoor transient particle transport simulations. Aerosol Sci. Tech. 49(10), 857-871.
Chen, C., Liu, W., Lin, C., Chen, Q., 2015b. Accelerating the Lagrangian method for modeling transient particle transport in indoor environments. Aerosol Sci. Tech. 49(5), 351-361.
Chen, C., Zhao, B., 2010. Some questions on dispersion of human exhaled droplets in ventilation room: Answers from numerical investigation. Indoor Air 20(2), 95-111.
Chen, Q., 1995. Comparison of different k-ε models for indoor air flow computations. Numerical Heat Transfer, Part B Fundamentals 28(3), 353-369.
Chen, Q., Srebric, J., 2002. A procedure for verification, validation, and reporting of indoor environment CFD analyses. HVAC&R Research 8(2), 201-216.
Chia, T., Ton, S., Liou, S., Hsu, H., Chen, C., Wan, G., 2019. Effectiveness of engineering interventions in decreasing worker exposure to metalworking fluid aerosols. Sci. Total Environ. 659, 923-927.
Choudhury, D. 1973. Introduction to the renormalization group method and turbulence modeling: Fluent incorporated.
Eisen, E. A., Smith, T. J., Kriebel, D., Woskie, S. R., Myers, D. J., Kennedy, S. M., Shalat, S., Monson, R. R., 2001. Respiratory health of automobile workers and exposures to metal‐working fluid aerosols: Lung spirometry. Am. J. Ind. Med. 39(5), 443-453.
Fisk, W. J., Rosenfeld, A. H., 1997. Estimates of improved productivity and health from better indoor environments. Indoor Air 7(3), 158-172.
GAMBIT 6.2 User's guide, 2005. GAMBIT 6.2 User's guide: Inc, Fluent.
Goldfield, J., 1985. Contaminant reduction: General vs. local exhaust ventilation. Heating, Piping and Air Conditioning 57(2), 47-51.
Holmberg, S., Li, Y., 1998. Modelling of the indoor environment — Particle dispersion and deposition. Indoor Air 8(2), 113-122.
Kukkonen, J., Vesala, T., Kulmala, M., 1989. The interdependence of evaporation and settling for

airborne freely falling droplets. J. Aerosol Sci. 20(7), 749-763.
Lacasse, Y., Girard, M., Cormier, Y., 2012. Recent advances in hypersensitivity pneumonitis. Chest 142(1), 208-217.
Lau, J., Chen, Q., 2007. Floor-supply displacement ventilation for workshops. Build. Environ. 42(4), 1718-1730.
Li, A., Ahmadi, G., 1992. Dispersion and deposition of spherical particles from point sources in a turbulent channel flow. Aerosol Sci. Tech. 16(4), 209-226.
Li, Y., Sandberg, M., Fuchs, L., 1992. Vertical temperature profiles in rooms ventilated by displacement: Full scale measurement and nodal modelling. Indoor Air 2(4), 225-243.
Lin, Y., Lin, C. L., 2014. A study on flow stratification in a space using displacement ventilation. Int. J. Heat Mass Tran. 73, 67-75.
Lin, Y., Wu, J. Y., 2017. A study on density stratification by mechanical extraction displacement ventilation. Int. J. Heat Mass Tran. 110, 447-459.
Mead-Hunter, R., King, A. J., Mullins, B. J., 2014. Aerosol-mist coalescing filters — A review. Sep. Purif. Technol. 133, 484-506.
Mirer, F. E., 2010. New evidence on the health hazards and control of metalworking fluids since completion of the OSHA advisory committee report. Am. J. Ind. Med. 53(8), 792-801.
Moon, J. H., Cho, D. H., Kang, S. Y., Choi, C. H., Im, Y. C., Lee, J. H., 2005. Improvement of Indoor Air Environment in a Large Welding Factory by Displacement Ventilation. Proceedings of the SAREK, 69-74.
National Institute for Occupational Safety and Health (NIOSH): Criteria for a Recommended Standard: Occupational Exposure to Metalworking Fluids. (98-102). Cincinnati,Ohio.
Nielsen, P. V., 1974. Flow in air conditioned rooms: Model experiments and numerical solution of the flow equations.
Nielsen, P. V., Mathisen, H. M., Moser, A. 2004. Ventilation effectiveness: Rehva.
O'Brien, D. M., 2003. Aerosol mapping of a facility with multiple cases of hypersensitivity pneumonitis: Demonstration of mist reduction and a possible dose/response relationship. Applied Occupational and Environmental Hygiene 18(11), 947-952.
Patankar, S. 2018. Numerical Heat Transfer and Fluid Flow: CRC press.
Rim, K., Lim, C., 2014. Biologically hazardous agents at work and efforts to protect workers' health: a review of recent reports. Safety and Health at Work 5(2), 43-52.
Wang, H., Huang, C., Liu, D., Zhao, F., Sun, H., Wang, F., Li, C., Kou, G., Ye, M., 2012. Fume transports in a high rise industrial welding hall with displacement ventilation system and individual ventilation units. Build. Environ. 52, 119-128.
Wang, H., Zhai, Z. J., 2016. Advances in building simulation and computational techniques: A review between 1987 and 2014. Energ. Buildings 128, 319-335.
Wang, M., Chen, Q., 2009. Assessment of various turbulence models for transitional flows in an enclosed environment (RP-1271). HVAC&R Research 15(6), 1099-1119.
Wang, M., Lin, C., Chen, Q., 2012. Advanced turbulence models for predicting particle transport in enclosed environments. Build. Environ. 47, 40-49.
Woskie, S. R., Smith, T. J., Hallock, M. F., Hammond, S. K., Rosenthal, F., Eisen, E. A., Kriebel, D., Greaves, I. A., 1994. Size-selective pulmonary dose indices for metal-working fluid aerosols in machining and grinding operations in the automobile manufacturing industry. American Industrial Hygiene Association Journal 55(1), 20-29.

Yakhot, V., Orszag, S. A., 1986. Renormalization group analysis of turbulence. I. Basic theory. J. Sci. Comput. 1(1), 3-51.
Yuan, X., Chen, Q., Glicksman, L. R., Hu, Y., Yang, X., 1999. Measurements and computations of room airflow with displacement ventilation. Ashrae Transactions 105, 340.
Zhai, Z. J., Zhang, Z., Zhang, W., Chen, Q. Y., 2007. Evaluation of various turbulence models in predicting airflow and turbulence in enclosed environments by CFD: Part 1 Summary of prevalent turbulence models. HVAC&R Research 13(6), 853-870.
Zhang, J., Long, Z., Liu, W., Chen, Q., 2016. Strategy for studying ventilation performance in factories. Aerosol Air Qual. Res. 16(2), 442-452.
Zhang, J., Shao, Y., Long, Z., 2016. Physicochemical characterization of oily particles emitted from different machining processes. J. Aerosol Sci. 96, 1-13.
Zhang, Z., Chen, Q., 2006. Experimental measurements and numerical simulations of particle transport and distribution in ventilated rooms. Atmos. Environ. 40(18), 3396-3408.
Zhang, Z., Chen, Q., 2007. Comparison of the Eulerian and Lagrangian methods for predicting particle transport in enclosed spaces. Atmos. Environ. 41(25), 5236-5248.
Zhang, Z., Zhang, W., Zhai, Z. J., Chen, Q. Y., 2007. Evaluation of various turbulence models in predicting airflow and turbulence in enclosed environments by CFD: Part 2 Comparison with experimental data from literature. HVAC&R Research 13(6), 871-886.
Zhao, B., Chen, C., Tan, Z., 2009. Modeling of ultrafine particle dispersion in indoor environments with an improved drift flux model. J. Aerosol Sci. 40(1), 29-43.
Zhu, Y., Zhao, B., Zhou, B., Tan, Z., 2012. A particle resuspension model in ventilation ducts. Aerosol Sci. Tech. 46(2), 222-235.